Research Square

Preprints are preliminary reports that have not undergone peer review.
They should not be considered conclusive, used to inform clinical practice,
or referenced by the media as validated information.

EPHX3 Drives Malignant Progression and Remodels the Immune Microenvironment in Gastric Adenocarcinoma

Hao Hu
Guizhou Provincial People's Hospital
Shaomin Cheng
Guizhou Provincial People's Hospital
Haitao Jiang
Guizhou Provincial People's Hospital
Danlian Tian
Guizhou Provincial People's Hospital
Xin Mao
Guizhou Provincial People's Hospital
Juan Du
Guizhou Provincial People's Hospital
Yufei Guan
Guizhou Provincial People's Hospital
Jiemin Liu
Guizhou Provincial People's Hospital
Jianlin Zhu
zeeheng210623@163.com

Guizhou Provincial People's Hospital

Article

Keywords: EPHX3, Gastric adenocarcinoma, PI3K/AKT, WNT signaling, Tumor microenvironment, Drug sensitivity

Posted Date: June 16th, 2026

DOI: https://doi.org/10.21203/rs.3.rs-9772440/v1

License: This work is licensed under a Creative Commons Attribution 4.0 International License.
Read Full License

Additional Declarations: No competing interests reported.

Abstract

Gastric adenocarcinoma (GA) remains a leading cause of cancer-related mortality worldwide, necessitating the identification of robust biomarkers for prognosis and therapy. While epoxide hydrolase 3 (EPHX3) has been implicated in xenobiotic metabolism, its role in GA is poorly defined. Herein, we demonstrate that EPHX3 is markedly upregulated in GA tissues and correlates with dismal clinical outcomes. Functional assays revealed that EPHX3 depletion suppresses cellular proliferation, migration, and invasion in vitro. Mechanistically, EPHX3 activates the PI3K/AKT and WNT signaling cascades. Furthermore, elevated EPHX3 expression reshapes the tumor immune microenvironment by impairing $CD8^+$ T cell infiltration while promoting M2 macrophage polarization. High EPHX3 levels also correlated with altered expression of immune checkpoints and predicted sensitivity to specific anti-neoplastic agents. Collectively, our findings position EPHX3 as a promising therapeutic target and prognostic indicator for GA.

1 Introduction

Gastric adenocarcinoma (GA) persists as a predominant global oncology challenge, ranking among the leading causes of cancer-related mortality[1]. A major contributor to this dismal outcome is the disease's insidious onset, which often culminates in diagnoses at advanced stages characterized by extensive local invasion and distant metastasis[2, 3]. Although multimodal therapeutic strategies, including radical gastrectomy, perioperative chemotherapy, and immune checkpoint inhibitors, the clinical benefits for patients with advanced disease remain marginal, with five-year survival rates stagnating below 30% [4–6]. This therapeutic bottleneck is largely attributed to the heterogeneous nature of GA and the inevitable emergence of drug resistance[7–9]. Consequently, there is an urgent imperative to elucidate the precise molecular circuitry governing GA progression and to identify novel, actionable biomarkers that can refine risk stratification and targeted therapy.

Epoxide hydrolases (EHs) constitute a superfamily of enzymes that catalyze the hydrolysis of highly reactive epoxides into less toxic diols[10, 11]. Beyond their canonical role in xenobiotic detoxification, emerging evidence implicates EHs in the regulation of endogenous signaling molecules, particularly bioactive lipid metabolites[12]. Among these, epoxide hydrolase 3 (EPHX3)—also referred to as soluble epoxide hydrolase-like—has remained relatively enigmatic compared to its paralogs. Recent transcriptomic profiling has identified EPHX3 dysregulation across a spectrum of malignancies, including neck squamous cell carcinoma, nasopharyngeal carcinoma and colorectal cancers, where it appears to modulate tumor cell proliferation and metastatic dissemination[13–15]. However, the specific expression landscape, biological function, and prognostic value of EPHX3 in the context of gastric carcinogenesis remain largely unexplored.

The tumor immune microenvironment (TIME) has emerged as a decisive factor influencing both disease progression and therapeutic response[16, 17]. Within the complex stromal ecosystem of GA, the balance between cytotoxic immunity and immunosuppression dictates clinical outcomes[18, 19]. Notably, the

PI3K/AKT and WNT/β-catenin signaling cascades represent two of the most frequently hyperactivated oncogenic pathways in GA[20, 21]. These pathways not only drive cell-autonomous proliferation but also intricately crosstalk with the immune stroma to foster an immunosuppressive niche[22, 23]. Whether EPHX3 interfaces with these critical signaling hubs to coordinate both tumor cell intrinsic growth and extrinsic immune evasion in GA remains a compelling question.

In this study, we hypothesize that EPHX3 functions as a pivotal oncogenic driver in GA. Through integrated bioinformatics analysis and rigorous in vitro validation, we aim to delineate the impact of EPHX3 on malignant phenotypes, uncover its regulatory role in the PI3K/AKT and WNT pathways, and evaluate its potential in remodeling immune cell infiltration. Our findings seek to establish EPHX3 as a novel prognostic indicator and a promising therapeutic target for overcoming the current impasse in GA management.

2 Materials and Methods

2.1 Bioinformatics analysis

The expression data of EPHX3 across pan-cancer and in GA tissues were downloaded from The Cancer Genome Atlas (TCGA) database. The expression difference of EPHX3 between GA tissues and normal gastric mucosal epithelium was analyzed using the limma package in R software. The correlation between EPHX3 expression and patient overall survival (OS), disease-specific survival (DSS), and progression-free survival (PFS) was evaluated using Kaplan-Meier survival analysis and log-rank test. The Human Protein Atlas (HPA) database was used to verify the protein expression level of EPHX3 in GA tissues. The association between EPHX3 expression and clinicopathological characteristics of GA patients was analyzed using chi-square test or Fisher's exact test.

GO (Gene Ontology) and KEGG (Kyoto Encyclopedia of Genes and Genomes) pathway enrichment analyses were performed using the clusterProfiler package in R software to explore the potential biological functions and signaling pathways of EPHX3. The Xcell and CIBERSORT algorithms were used to analyze the correlation between EPHX3 expression and immune cell infiltration in GA tissues. The correlation between EPHX3 expression and immune checkpoint molecules, TMB, and MSI was analyzed using Pearson correlation analysis. The TIDE (Tumor Immune Dysfunction and Exclusion) score was used to predict the association between EPHX3 expression and immunotherapy response. The correlation between EPHX3 expression and drug sensitivity was analyzed using the GDSC (Genomics of Drug Sensitivity in Cancer) database.

2.2 Cell Culture and transfection

Human GA cell lines (GSU, NUGC-4, MKN7 and AGS) and normal gastric epithelial cell line (GES1) were purchased from the Cell Bank of Chinese Academy of Sciences (Shanghai, China). All cells were cultured in RPMI 1640 medium (Gibco, USA) supplemented with 10% fetal bovine serum (FBS, Gibco, USA) and 1% penicillin-streptomycin (Gibco, USA) at 37°C in a humidified atmosphere with 5% CO_2. The short

hairpin RNA (shRNA) targeting EPHX3 (shEPHX3) and negative control shRNA (shctrl) were synthesized by GenePharma (Shanghai, China). Cell transfection was performed using Lipofectamine 3000 (Invitrogen, USA) according to the manufacturer's instructions. Stable EPHX3 knockdown cell lines were established by puromycin selection (2 μg/mL) for 2 weeks.

2.3 Quantitative Real-Time PCR (qPCR)

Total RNA was extracted from cells using Trizol reagent (Invitrogen, USA) according to the manufacturer's protocol. The cDNA was synthesized using the PrimeScript RT Reagent Kit (TaKaRa, Japan). qPCR was performed using the SYBR Premix Ex Taq II Kit (TaKaRa, Japan) on a StepOnePlus Real-Time PCR System (Applied Biosystems, USA). GAPDH was used as an internal reference. The relative expression level of EPHX3 was calculated using the $2^{-\Delta\Delta Ct}$ method. The primer sequences were as follows: EPHX3 forward: 5'-TCACAGCACTGGCATTGGAA-3', reverse: 5'-GCCACTTAATGCTCCAGGCT-3'; GAPDH forward: 5'-TGGAAATCCCATCACCATCT-3', reverse: 5'-TGGACTCCACGACGTACTCA-3'.

2.4 Western Blotting (WB)

Total protein was extracted from cells using RIPA lysis buffer (Beyotime, China) containing protease inhibitor and phosphatase inhibitor. The protein concentration was determined using the BCA Protein Assay Kit (Beyotime, China). Equal amounts of protein were separated by 10% SDS-PAGE and transferred to PVDF membranes (Millipore, USA). The membranes were blocked with 5% non-fat milk for 1 hour at room temperature, then incubated with primary antibodies overnight at 4°C. After washing with TBST, the membranes were incubated with secondary antibody for 1 hour at room temperature. The protein bands were visualized using the ECL Chemiluminescence Kit (Beyotime, China) and imaged using the ChemiDoc XRS+ Imaging System (Bio-Rad, USA). The relative protein expression level was quantified using ImageJ software.

2.5 Cell Viability Assay

Cell viability was detected using the CCK-8 assay (Beyotime, China). Briefly, cells were seeded in 96-well plates at a density of 2×10^3 cells per well. After 24, 48, and 72 hours of culture, 10 μL of CCK-8 solution was added to each well and incubated for 2 hours at 37°C. The absorbance at 450 nm was measured using a microplate reader (Thermo Fisher Scientific, USA). Each experiment was performed in triplicate.

2.6 Colony Formation Assay

Cells were seeded in 6-well plates at a density of 500 cells per well and cultured for 7 days. The colonies were fixed with 4% paraformaldehyde for 15 minutes, stained with 0.1% crystal violet for 10 minutes, and washed with PBS. The number of colonies with more than 50 cells was counted under a microscope. Each experiment was performed in triplicate.

2.7 Transwell assay

The transwell assay was used to detect cell migration and invasion capacity. For the migration assay, cells were seeded in the upper chamber of transwell inserts (8 μm pore size, Corning, USA) in serum-free

medium. The lower chamber was filled with medium containing 10% FBS. After 24 hours of culture, the cells on the upper surface of the membrane were removed with a cotton swab, and the cells on the lower surface were fixed with 4% paraformaldehyde and stained with 0.1% crystal violet. The number of migrated cells was counted under a microscope. For the invasion assay, the upper chamber was pre-coated with Matrigel (BD Biosciences, USA) and then seeded with cells, and the rest of the steps were the same as the migration assay. Each experiment was performed in triplicate.

2.8 Immunohistochemical (IHC) staining

GA tissues and paired normal tissues were obtained from patients who underwent surgical resection at our hospital. The tissues were fixed with 4% paraformaldehyde, embedded in paraffin, and sectioned into 4 μm thick slices. The sections were deparaffinized, rehydrated, and subjected to antigen retrieval. After blocking with 5% BSA, the sections were incubated with primary antibodies (anti-EPHX3, anti-CD8, anti-CD206) overnight at 4°C. Then, the sections were incubated with secondary antibody and stained with DAB. The sections were counterstained with hematoxylin, dehydrated, and mounted. The staining intensity was evaluated by two independent pathologists. The final score was the product of the staining intensity and positive rate, and samples with a score ≥ 4 were considered high expression.

2.9 Statistical Analysis

All statistical analyses were performed using SPSS 22.0 software and R software (version 4.2.0). The data were presented as mean ± standard deviation (SD). The differences between two groups were compared using t-test, and the differences among multiple groups were compared using one-way ANOVA. The correlation between EPHX3 expression and clinicopathological characteristics was analyzed using chi-square test or Fisher's exact test. The survival curves were plotted using Kaplan-Meier method, and the log-rank test was used to compare the survival differences. Pearson correlation analysis was used to analyze the correlation between EPHX3 expression and immune cell infiltration, immune checkpoint molecules, TMB, and MSI. $P < 0.05$ was considered statistically significant.

3 Results

3.1 EPHX3 is highly expressed in GA and correlated with poor prognosis

Systematic interrogation of the TCGA pan-cancer dataset revealed that EPHX3 is broadly upregulated across various malignant lineages, with gastric adenocarcinoma exhibiting particularly pronounced expression levels (Fig. 1A). Quantitative analysis confirmed that EPHX3 transcripts were significantly enriched in tumor tissues compared to normal gastric mucosa (Fig. 1B). Crucially, survival analysis demonstrated that patients stratified into the high EPHX3 cohort experienced significantly shorter Overall Survival (OS), Disease-Specific Survival (DSS), and Progression-Free Survival (PFS) (Fig. 1C-E). We next validated these findings at the protein level using clinical specimens. Figure 1F presented representative immunohistochemical (IHC) images showing intense cytoplasmic staining for EPHX3 in

tumor tissues compared to adjacent normal tissues. Quantification of these samples confirmed a significant increase in EPHX3 protein expression in tumors versus paired normals (Fig. 1G). Figure 1H further illustrated the survival stratification, reinforcing that EPHX3 acts as a negative prognostic marker. Finally, Fig. 1I (antibody HPA012842) corroborates our IHC data with independent proteomic evidence from the Human Protein Atlas (https://www.proteinatlas.org/) database.These results suggest that EPHX3 is highly expressed in GA and may serve as a poor prognostic biomarker for GA patients.

3.2 EPHX3 Expression is Correlated with Clinicopathological Characteristics of GA Patients

We further analyzed the association between EPHX3 expression and clinicopathological characteristics of GA patients. The results showed that EPHX3 expression was not significantly correlated with patient age, gender, or race (Figs. 2A-C). However, EPHX3 expression was closely associated with pathological staging of GA patients, including histological grade, TNM stage, and tumor invasion status (Figs. 2D-F). Specifically, EPHX3 expression was significantly higher in GA patients with advanced histological grade, advanced TNM stage, and high tumor invasion status. To dissect this further, we analyzed specific staging parameters. Figures 2G-I illustrated that EPHX3 expression increases progressively with advancing T classification (tumor size/depth), N classification (lymph node metastasis), and M classification (distant metastasis), respectively. These data suggest that EPHX3 is linked to the acquisition of metastatic potential.

3.3 Genetic depletion of EPHX3 impairs malignant cellular phenotypes

To define the functional role of EPHX3in GA, we first detected the expression level of EPHX3 in multiple GA cell lines (GSU, NUGC-4, MKN7) and normal gastric epithelial cell line (GES1). The qPCR and WB results showed that EPHX3 was highly expressed in GA cell lines compared with GES1 cells, and GSU and NUGC-4 cells had relatively high EPHX3 expression (Figs. 3A and B). Therefore, we chose GSU and NUGC-4 cells for subsequent experiments. We successfully constructed EPHX3 knockdown cell lines (shEPHX3) using shRNA transfection, and the knockdown efficiency was verified by qPCR and WB (Figs. 3C and D). Functionally, Fig. 3E demonstrates that EPHX3 silencing significantly reduces cell viability. The colony formation assay showed that the number of colonies formed by shEPHX3 cells was significantly less than that of shctrl cells, indicating that EPHX3 knockdown impaired the clonogenic capacity of GA cells (Fig. 3F). The transwell assay showed that knockdown of EPHX3 significantly reduced the migration and invasion abilities of GSU and NUGC-4 cells (Figs. 3G and H). These results suggest that EPHX3 plays an oncogenic role in GA by promoting cell proliferation, migration, and invasion.

3.4 EPHX3 mediates the activation of PI3K/AKT and WNT signaling pathways in GA

To elucidate the underlying molecular mechanism of EPHX3 in GA, we performed GO and KEGG pathway enrichment analyses. The GO analysis showed that EPHX3-related genes were mainly enriched inWnt pathway-driven dysregulation of epithelial cell differentiation, Extracellular Matrix (ECM) remodeling, protease system imbalance, and inflammatory-immune disorders, which together constitute the core oncogenic program driving tumor invasion and metastasis (Figs. 4A). Figure 4B presents the KEGG pathway enrichment, which identified significant enrichment of the PI3K/AKT and WNT signaling pathways among EPHX3-correlated genes. We intended to further verify the effect of EPHX3 on PI3K/AKT and WNT signaling pathways using western blotting. The results showed that knockdown of EPHX3 significantly reduced the phosphorylation levels of PI3K and AKT, but had no significant effect on the total protein levels of PI3K and AKT (Fig. 4C). Similarly, Fig. 4D demonstrates that EPHX3 depletion suppressed WNT pathway activity, as indicated by reduced phosphorylation of β-catenin. These results confirm that EPHX3 mediates the activation of PI3K/AKT and WNT signaling pathways in GA.

3.5 EPHX3 is involved in immune cell infiltration in GA

To explore the role of EPHX3 in the immune microenvironment of GA, we analyzed the correlation between EPHX3 expression and immune cell infiltration using Xcell and CIBERSORT algorithms. The results of Xcell algorithm showed that EPHX3 expression was significantly correlated with the infiltration of various immune cells in GA tissues, including T cells CD4 memory activated, Macrophages M1, Dendritic cells activated and T cells CD8 (Figs. 5A-D). The results of CIBERSORT algorithm further confirmed that EPHX3 expression was closely associated with immune cell infiltration in GA tissues, including Myeloid dendritic cell activated, T cell $CD8^+$, T cell $CD4^+$ memory and T cell $CD8^+$ naive (Figs. 5E-H). To validate these in silico findings, we performed IHC staining on clinical tissues. Figures 5I and J illustrated that tumors with low EPHX3 expression exhibit dense infiltration of $CD8^+$T cells, whereas Figs. 5K and L show that high EPHX3 expression is associated with increased infiltration of $CD206^+$ M2 macrophages. These results suggest that EPHX3 is involved in regulating immune cell infiltration in GA tissues, which may affect the immune microenvironment of GA.

3.6 EPHX3 expression is correlated with immune signatures and drug sensitivity in GA

We further analyzed the correlation between EPHX3 expression and immune signatures in GA. The butterfly plot results showed that EPHX3 expression was significantly correlated with the expression of immune checkpoint molecules, including immune activators and inhibitors (Figs. 6A and B). Figures 6C and D demonstrated that EPHX3 levels are significantly correlated with key immune biomarkers, specifically Tumor Mutational Burden (TMB) and Microsatellite Instability (MSI). The TIDE score analysis showed that GA patients with high EPHX3 expression had higher TIDE scores, indicating that they may have poor response to immunotherapy (Fig. 6E).

In addition, we analyzed the correlation between EPHX3 expression and drug sensitivity using the GDSC database (Genomics of Drug Sensitivity in Cancer, www.cancerrxgene.org). The results showed that patients with high EPHX3 expression exhibited reduced sensitivity to AZD6244 and Camptothecin

(Fig. 7A and B). In contrast, high EPHX3 expression was associated with increased sensitivity to multiple other agents, including GNF-2, AZD6482, ABT-263, AMG-706, AZD0530, FH535, Imatinib, and CCT007093 (Fig. 7C-L). These results imply that EPHX3 may be a potential predictor of drug sensitivity in GA.

4 Discussion

Despite incremental advances in surgical techniques and systemic therapies, the prognosis for patients with advanced GA remains grim[24, 25]. The identification of novel molecular drivers is therefore paramount. In this study, we systematically investigated the expression pattern, biological function, and underlying molecular mechanisms of EPHX3 in GA, and explored its correlation with immune microenvironment, immune signatures, and drug sensitivity. Our findings demonstrate that EPHX3 is highly expressed in GA tissues and is closely associated with poor prognosis and malignant progression of GA patients, suggesting that EPHX3 may serve as a potential oncogenic biomarker and therapeutic target for GA.

Previous studies have shown that EPHX3 is abnormally expressed in various cancers and plays an important role in tumor progression. For example, EPHX3 is highly expressed in nasopharyngeal carcinoma and promotes tumor cell proliferation and migration by regulating the Wnt/β-Catenin signaling pathway[14]. In colorectal cancer, EPHX3 is associated with tumor metastasis and poor prognosis[13]. Consistent with these studies, our results showed that EPHX3 is highly expressed in GA tissues and cell lines, and its high expression is associated with unfavorable prognosis of GA patients. In vitro experiments further confirmed that knockdown of EPHX3 suppresses the proliferation, migration, and invasion of GA cells, indicating that EPHX3 plays an oncogenic role in GA.

The PI3K/AKT and WNT signaling pathways are key oncogenic pathways that are frequently activated in GA and regulate various biological processes of tumor cells[14, 20]. Our KEGG pathway enrichment analysis showed that EPHX3-related genes are significantly enriched in these two pathways. WB results further confirmed that knockdown of EPHX3 reduces the phosphorylation levels of PI3K, AKT, and β-catenin, indicating that EPHX3 mediates the activation of PI3K/AKT and WNT signaling pathways in GA. These findings suggest that EPHX3 promotes GA progression by activating PI3K/AKT and WNT signaling pathways, which provides a new molecular mechanism for the oncogenic role of EPHX3 in GA.

An intriguing aspect of our findings is the role of EPHX3 in remodeling the tumor immune microenvironment (TIME). We observed that high EPHX3 expression correlates with a "cold" tumor phenotype—characterized by excluded $CD8^+$ T cells and enriched M2 macrophages. This aligns with recent literature suggesting that Wnt/β-catenin signaling can directly suppress T-cell priming and recruitment[26, 27]. By activating WNT signaling, EPHX3 may thus act as a molecular bridge linking intracellular oncogenic signaling to extrinsic immune evasion. This hypothesis is further supported by our TIDE analysis, which predicts that EPHX3-high patients are less likely to benefit from immune checkpoint blockade.

From a translational perspective, our study highlights EPHX3 as a potential predictive biomarker for drug sensitivity. The correlation between EPHX3 levels and differential responses to various anti-neoplastic agents suggests that EPHX3 status could guide precision medicine approaches. For instance, patients with high EPHX3 expression might be spared ineffective immunotherapy, while being directed toward specific chemotherapeutics to which they are sensitized.

This study has some limitations. However, this study is not without limitations. First, the precise biochemical mechanism by which EPHX3—an enzyme traditionally involved in lipid metabolism—activates kinase signaling remains to be elucidated. Future studies should investigate whether EPHX3 alters the levels of specific bioactive lipid mediators (e.g., epoxyeicosatrienoic acids) that in turn activate PI3K or WNT pathways. Second, while our in vitro data are robust, in vivo validation using patient-derived xenografts (PDX) or syngeneic mouse models is necessary to confirm the immunomodulatory role of EPHX3 in a physiologically relevant setting. Finally, the role of EPHX3 in GA immunotherapy and drug sensitivity needs to be verified by in vivo experiments and clinical trials.

In conclusion, our study establishes EPHX3 as a central node integrating oncogenic signaling, immune suppression, and therapeutic response in gastric adenocarcinoma. Targeting EPHX3 or its downstream effectors may represent a novel therapeutic avenue to overcome the current stagnation in GA treatment.

5 Conclusion

Collectively, this study establishes EPHX3 as a critical oncogenic driver in gastric adenocarcinoma, wherein its aberrant overexpression correlates with advanced pathological staging and dismal patient survival. We demonstrate that EPHX3 orchestrates malignant progression by enhancing cellular proliferation, migration, and invasion through the concerted activation of the PI3K/AKT and WNT/β-catenin signaling pathways. Beyond its cell-intrinsic roles, EPHX3 actively remodels the tumor immune microenvironment by suppressing $CD8^+$ T-cell infiltration and promoting M2 macrophage polarization, thereby fostering an immunosuppressive niche that correlates with high immune checkpoint expression and predicted resistance to immunotherapy. Furthermore, EPHX3 expression profiles stratify tumor sensitivity to various chemotherapeutic and targeted agents, highlighting its potential as a dual-purpose biomarker for prognosis and personalized therapeutic guidance in gastric adenocarcinoma.

Declarations

Ethics approval and consent to participate

The Medical Ethics committee of Guizhou Provincial People's Hospital approved all procedures performed in the present study involving human participants (approval no. 2026-091), which were in accordance with the Declaration of Helsinki, and all patients provided written informed consent prior to participation in this study.

Conflict of interest statement

All authors in this study declare that they have no conflict of interest.

Consent for publication

Not applicable.

Funding

This work was supported by Guizhou Provincial People's Hospital Talent Fund [2023]-20, Natural Science Foundation of Guizhou Province ZK[2024]-453, Natural Science Foundation of Guizhou Province MS[2026]-359 and Science and Technology Fund Project of the Health Commission of Guizhou Province gzwkj2026-028.

Author Contribution

Hao Hu spearheaded the conceptualization and strategic design of the study. Bioinformatic analyses were jointly executed by Shaomin Cheng and Haitao Jiang. The in vitro experimental validation was carried out by Haitao Jiang and Hao Hu. Statistical oversight and data interpretation were provided by Qian Du and Xin Mao. Acquisition of clinical specimens and resources was facilitated by Yufei Guan, Danlian Tian, and Juan Du. The original draft manuscript was written by Jianlin Zhu and Jiemin Liu, with subsequent critical revisions. All authors have read, revised, and approved the submitted manuscript and agree to be accountable for all aspects of the work.

Acknowledgement

Not applicable.

Data Availability

The transcriptomic data utilized in this study were retrieved from publicly accessible repositories. Specifically, The Cancer Genome Atlas (TCGA) dataset is available through the Genomic Data Commons (GDC) portal (https://portal.gdc.cancer.gov/). The Human Protein Atlas (HPA) data can be accessed via its official website (https://www.proteinatlas.org/). Additionally, all original data generated during this study, including raw Western blot images and immunohistochemistry scans, are available from the corresponding author upon reasonable request.

References

1. Patel, A. K., Sethi, N. S. & Park, H. *Gastric Cancer: Rev. JAMA*, **335** 439–450. (2026).

2. Joshi, S. S. & Badgwell, B. D. Current treatment and recent progress in gastric cancer. *CA Cancer J. Clin.* **71**, 264–279 (2021).
3. Kim, S. E., Park, M. I. & Lee, M. H. [Chemotherapy for Metastatic Gastric Cancer]. *Korean J. Gastroenterol.* **85**, 1–10 (2025).
4. Wang, Y. & Chong, G. Immunotherapy in gastric adenocarcinoma - a rapidly evolving treatment landscape. *Crit. Rev. Oncol. Hematol.* **216**, 104941 (2025).
5. Shah, M. A. et al. Zolbetuximab plus CAPOX in CLDN18.2-positive gastric or gastroesophageal junction adenocarcinoma: the randomized, phase 3 GLOW trial. *Nat. Med.* **29**, 2133–2141 (2023).
6. Taieb, J. et al. Treatment of gastric adenocarcinoma: A rapidly evolving landscape. *Eur. J. Cancer*. **195**, 113370 (2023).
7. Zhang, M. et al. Dissecting transcriptional heterogeneity in primary gastric adenocarcinoma by single cell RNA sequencing. *Gut* **70**, 464–475 (2021).
8. N. Cancer Genome Atlas Research, Comprehensive molecular characterization of gastric adenocarcinoma. *Nature*, **513** 202–209. (2014).
9. Zhao, P. et al. HKDC1 reprograms lipid metabolism to enhance gastric cancer metastasis and cisplatin resistance via forming a ribonucleoprotein complex. *Cancer Lett.* **569**, 216305 (2023).
10. Bucko, M., Kaniakova, K., Hronska, H., Gemeiner, P. & Rosenberg, M. Epoxide Hydrolases: Multipotential Biocatalysts, Int J Mol Sci, 24 (2023).
11. Fretland, A. J. & Omiecinski, C. J. Epoxide hydrolases: biochemistry and molecular biology. *Chem. Biol. Interact.* **129**, 41–59 (2000).
12. Blum, M., Dogan, I., Karber, M., Rothe, M. & Schunck, W. H. Chiral lipidomics of monoepoxy and monohydroxy metabolites derived from long-chain polyunsaturated fatty acids. *J. Lipid Res.* **60**, 135–148 (2019).
13. Cao, L. et al. The prognostic significance of epoxide hydrolases in colorectal cancer. *Biochem. Biophys. Rep.* **41**, 101912 (2025).
14. Hong, Q. et al. Effect of MicroRNA-4713-3p on Promoting Malignant Progression of Nasopharyngeal Carcinoma via Targeted Inhibition of EPHX3 to Activate Wnt/beta-Catenin Signaling Pathway. *J. Biochem. Mol. Toxicol.* **39**, e70450 (2025).
15. Ding, S. et al. miRNA-Mediated Low Expression of EPHX3 Is Associated with Poor Prognosis and Tumor Immune Infiltration in Head and Neck Squamous Cell Carcinomas, J Oncol, (2022) 7633720. (2022).
16. Lei, X. et al. Immune cells within the tumor microenvironment: Biological functions and roles in cancer immunotherapy. *Cancer Lett.* **470**, 126–133 (2020).
17. Aliazis, K. et al. The tumor microenvironment's role in the response to immune checkpoint blockade. *Nat. Cancer*. **6**, 924–937 (2025).
18. Sattiraju, A. et al. Hypoxic niches attract and sequester tumor-associated macrophages and cytotoxic T cells and reprogram them for immunosuppression. *Immunity* **56**, 1825–1843e1826

(2023).
19. Fortin, B. M. et al. Circadian control of tumor immunosuppression affects efficacy of immune checkpoint blockade. *Nat. Immunol.* **25**, 1257–1269 (2024).
20. Morgos, D. T. et al. Targeting PI3K/AKT/mTOR and MAPK Signaling Pathways in Gastric Cancer. *Int. J. Mol. Sci.*, **25** (2024).
21. Wang, Y. et al. Wnt/beta-catenin signaling confers ferroptosis resistance by targeting GPX4 in gastric cancer. *Cell. Death Differ.* **29**, 2190–2202 (2022).
22. Sun, P. et al. SPTSSA facilitates gastric cancer progression with modulating PD-L1 in immunomicroenvironment through Wnt/beta-catenin pathway. *Cell. Oncol. (Dordr)*. **48**, 1127–1144 (2025).
23. Shi, T. et al. DKK1 Promotes Tumor Immune Evasion and Impedes Anti-PD-1 Treatment by Inducing Immunosuppressive Macrophages in Gastric Cancer. *Cancer Immunol. Res.* **10**, 1506–1524 (2022).
24. Zhang, J. et al. JiaoYang, High expression of SENP1 correlates with poor prognosis and immune evasion in gastric cancer. *Int. Immunopharmacol.* **167**, 115680 (2025).
25. Ding, L. et al. MCM8 promotes gastric cancer progression through RPS15A and predicts poor prognosis. *Cancer Med.* **13**, e7424 (2024).
26. Zhai, J. et al. ALKBH5 Drives Immune Suppression Via Targeting AXIN2 to Promote Colorectal Cancer and Is a Target for Boosting Immunotherapy, Gastroenterology, 165 445–462. (2023).
27. Garris, C. S. & Luke, J. J. Dendritic Cells, the T-cell-inflamed Tumor Microenvironment, and Immunotherapy Treatment Response. *Clin. Cancer Res.* **26**, 3901–3907 (2020).

Figures

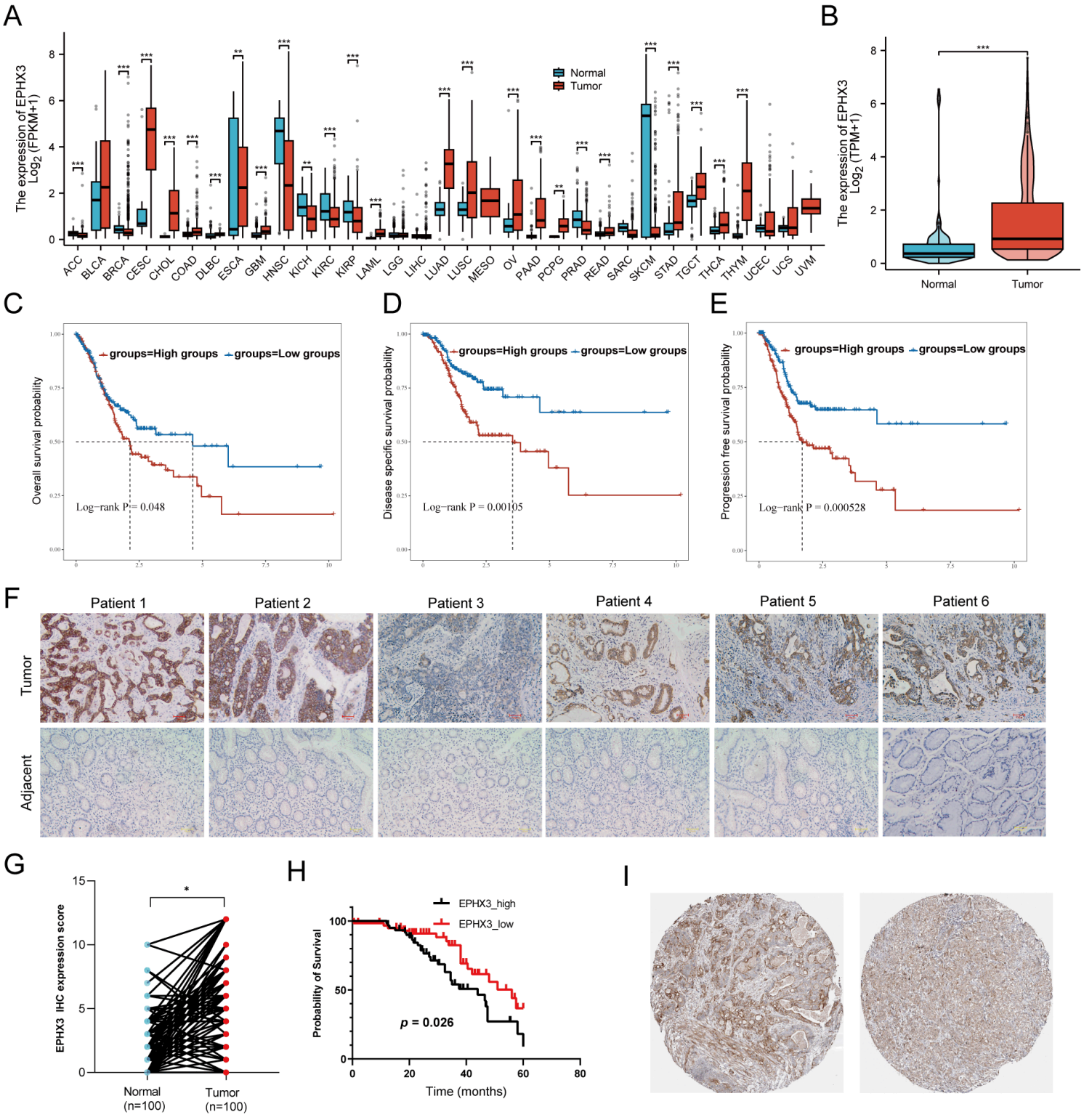


Figure 1

EPHX3 is highly expressed in GA and is closely associated with patient prognosis

(A) Expression profiles of EPHX3 across pan-cancer specimens based on TCGA database.
(B) Differential mRNA expression of EPHX3 between GA tissues and normal gastric mucosal epithelium.
(C-E) Correlations between EPHX3 expression levels and patient overall survival (OS), disease-specific

survival (DSS), and progression-free survival (PFS).(F) Immunohistochemical staining showing EPHX3 protein expression in GA and adjacent normal tissues. (G) Expression differences of EPHX3 between GA tissues and paired normal tissues. (H) Survival analyses of GA patients stratified by high and low EPHX3 expression. (I) EPHX3 expression status in the Human Protein Atlas (HPA) database.

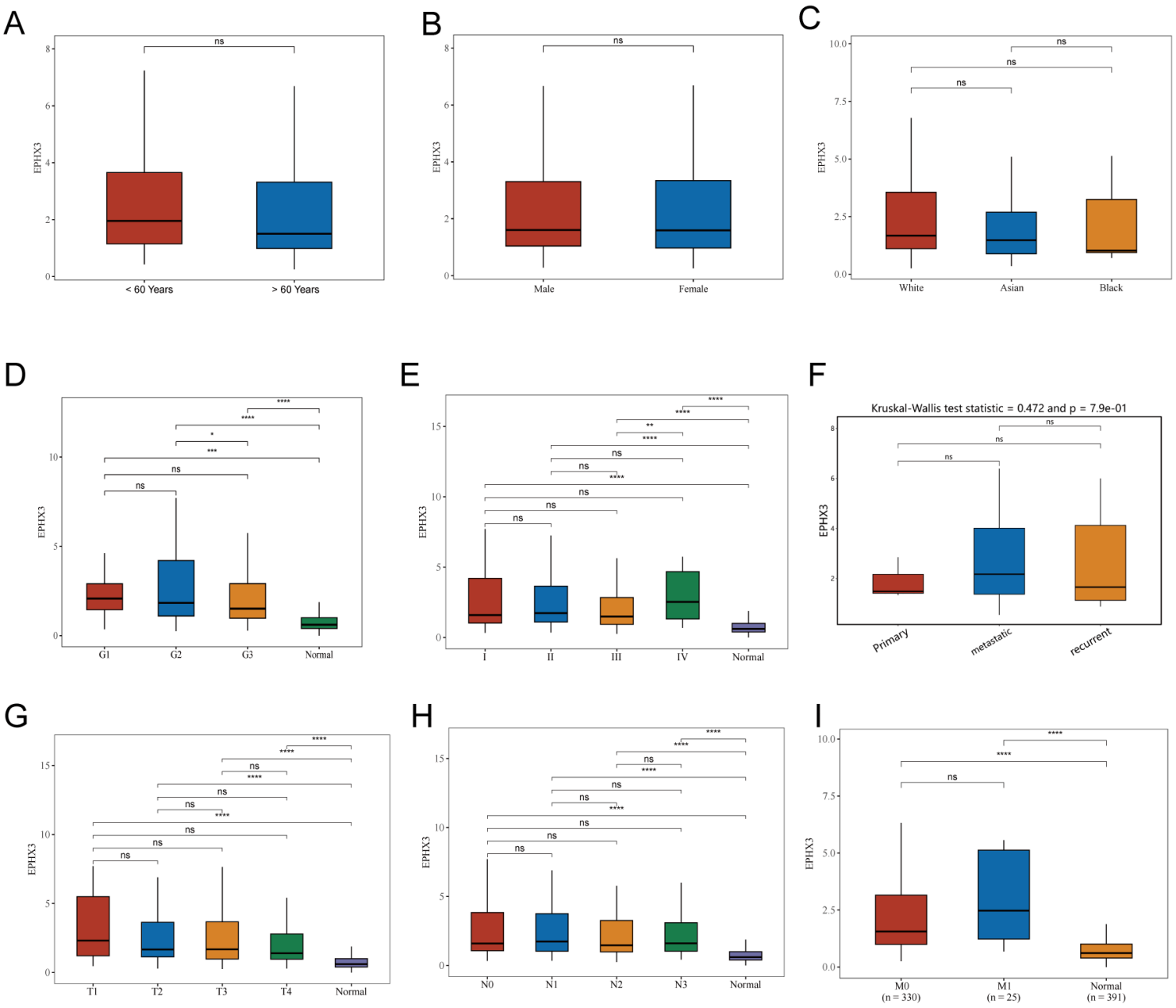


Figure 2

Correlation analysis between EPHX3 expression and clinicopathological characteristics of GA patients

(A-C) Associations of EPHX3 expression with patient age, gender, and race. (D-F) Correlations between EPHX3 expression and pathological staging, including histological grade, TNM stage, and tumor invasion status. (G-I) Expression differences of EPHX3 across distinct T, N, and M stages of GA.

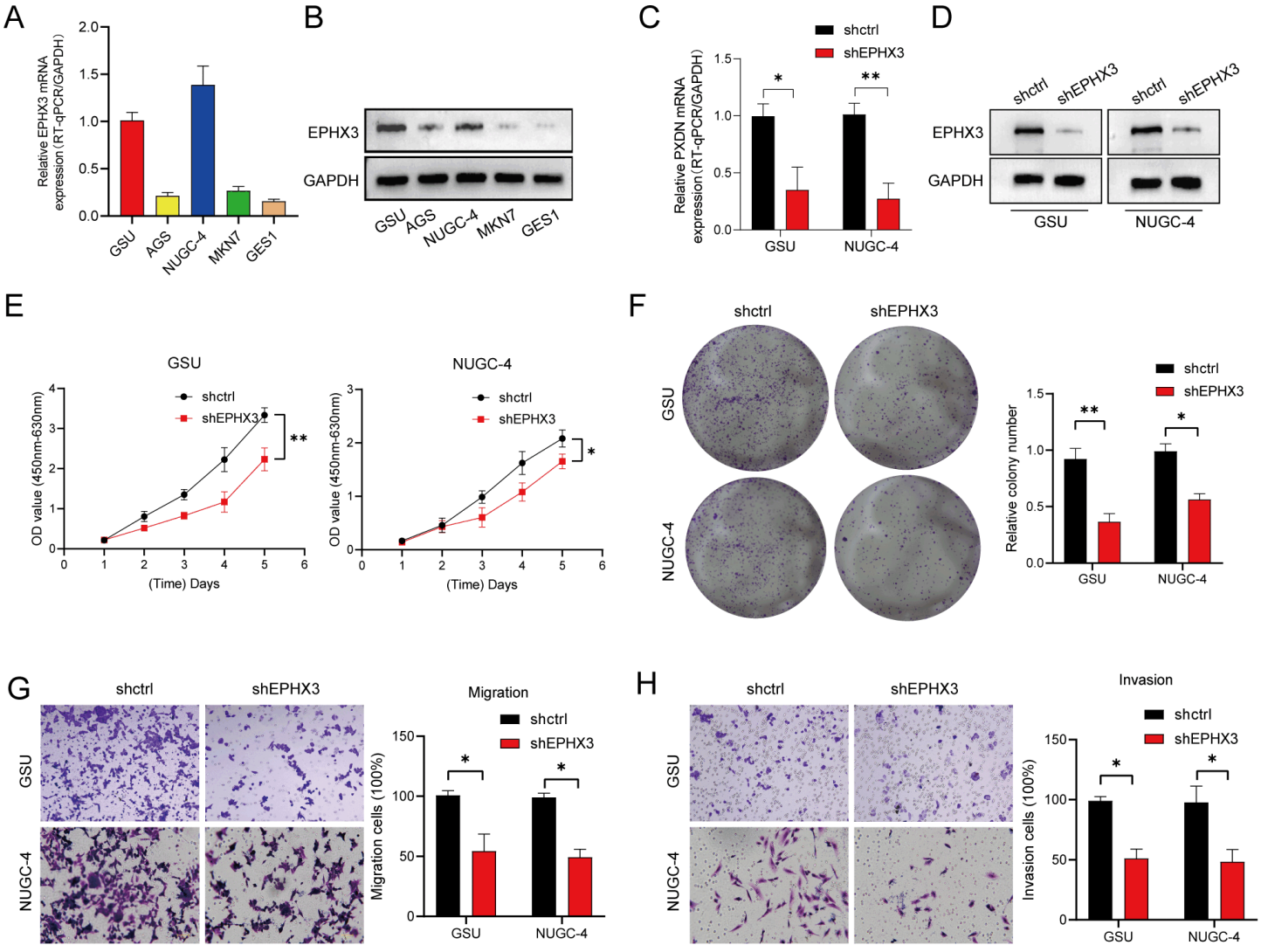


Figure 3

EPHX3 knockdown suppresses the proliferation, invasion, and migration of GA cells

(A, B) EPHX3 expression at mRNA and protein levels in multiple GA cell lines. (C, D) Validation of EPHX3 knockdown efficiency in gastric cancer cell lines using western blotting (WB) and quantitative real-time PCR (qPCR). (E) EPHX3 knockdown reduces the viability of GA cells. (F) EPHX3 knockdown impairs the clonogenic capacity of GA cells. (G, H) EPHX3 knockdown inhibits the migration and invasion of GA cells. Data are shown as mean ± SD from three independent experiments (n = 3).

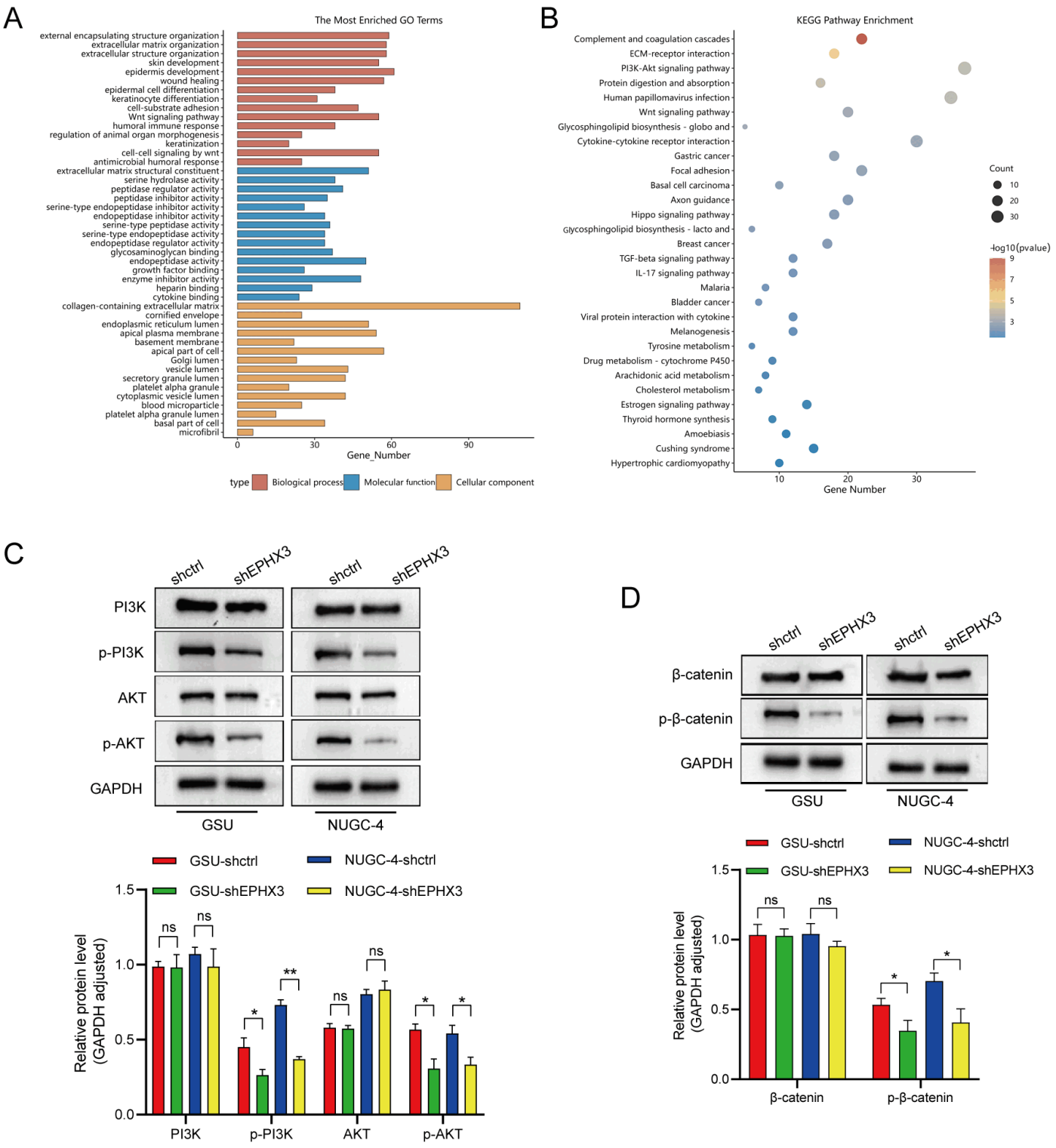


Figure 4

EPHX3 mediates the activation of PI3K/AKT and Wnt signaling pathways in GA

(A, B) Bioinformatic analyses of EPHX3-related biological functions using GO and KEGG pathway enrichment. (C) Western blotting analysis of PI3K/AKT signaling activity following EPHX3 knockdown.

(D) Western blotting analysis of Wnt signaling activity following EPHX3 knockdown. Data are shown as mean ± SD from three independent experiments (n = 3).

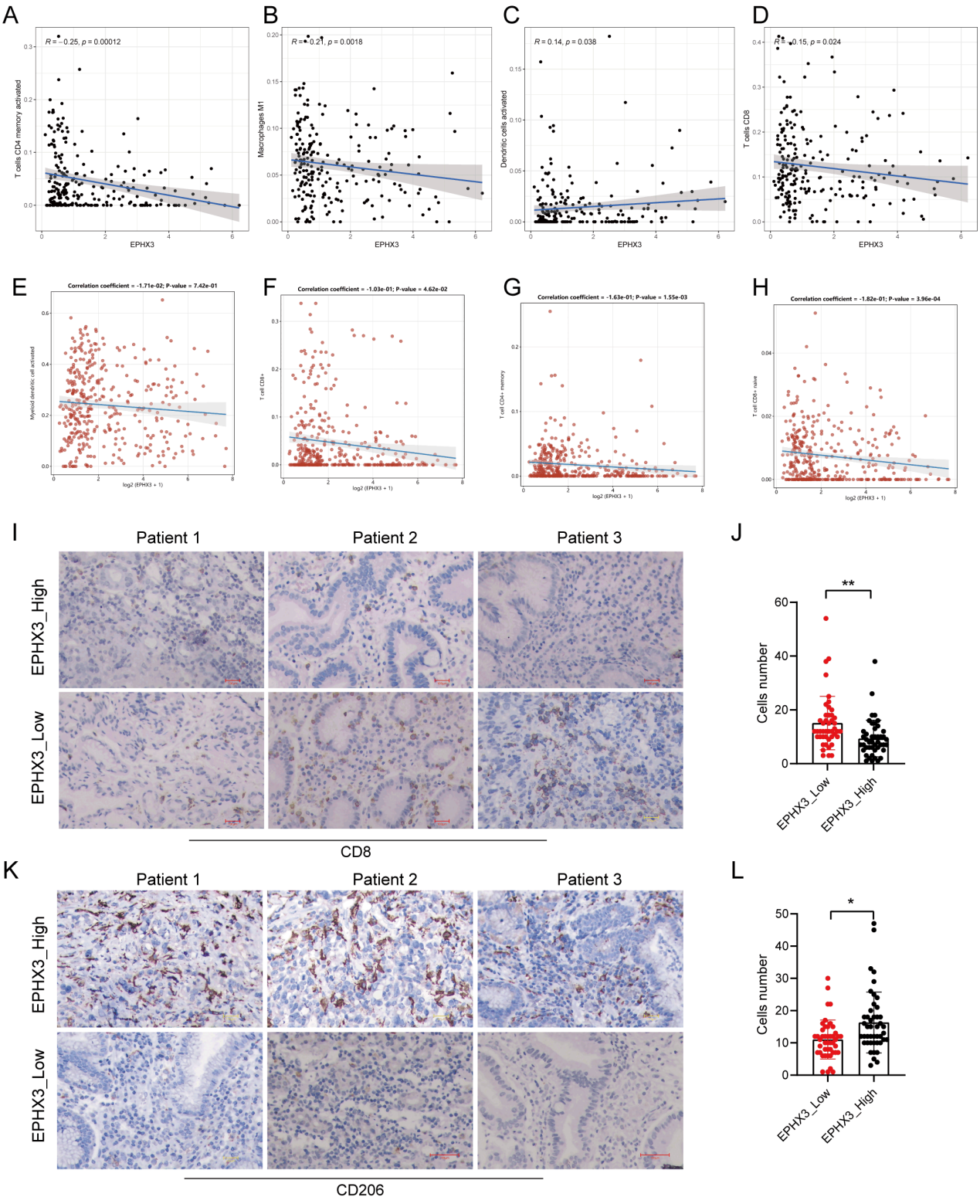


Figure 5

EPHX3 is involved in immune cell infiltration in GA tissues

(A-D) Correlations between EPHX3 expression and immune cell infiltration in GA analyzed by Xcell algorithm. (E-H) Associations of EPHX3 expression with immune cell infiltration in GA evaluated by CIBERSORT algorithm. (I, J) Immunohistochemical analysis of the effect of EPHX3 expression on $CD8^+$ T cell infiltration in GA tissues. (K, L) Immunohistochemical assessment of the impact of EPHX3 expression on M2 macrophage infiltration in GA tissues.

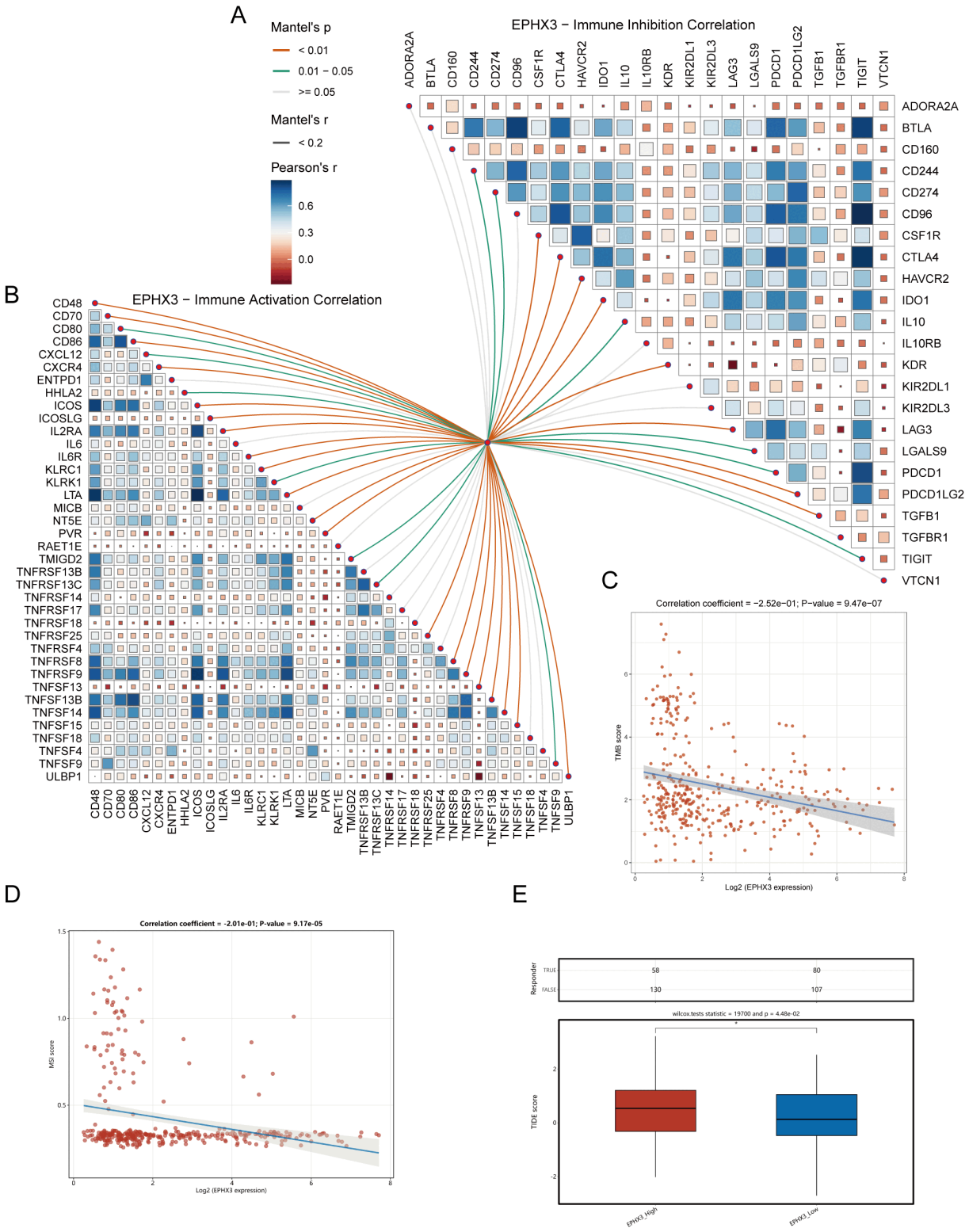


Figure 6

Correlation between EPHX3 expression and immune signatures in GA

(A, B) Butterfly plots illustrating the associations of EPHX3 expression with immune checkpoint molecules, including immune activators and inhibitors. (C, D) Correlations of EPHX3 expression with immune response biomarkers, including tumor mutational burden (TMB) and microsatellite instability (MSI). (E) Association between EPHX3 expression and immunotherapy response predicted by TIDE scoring.

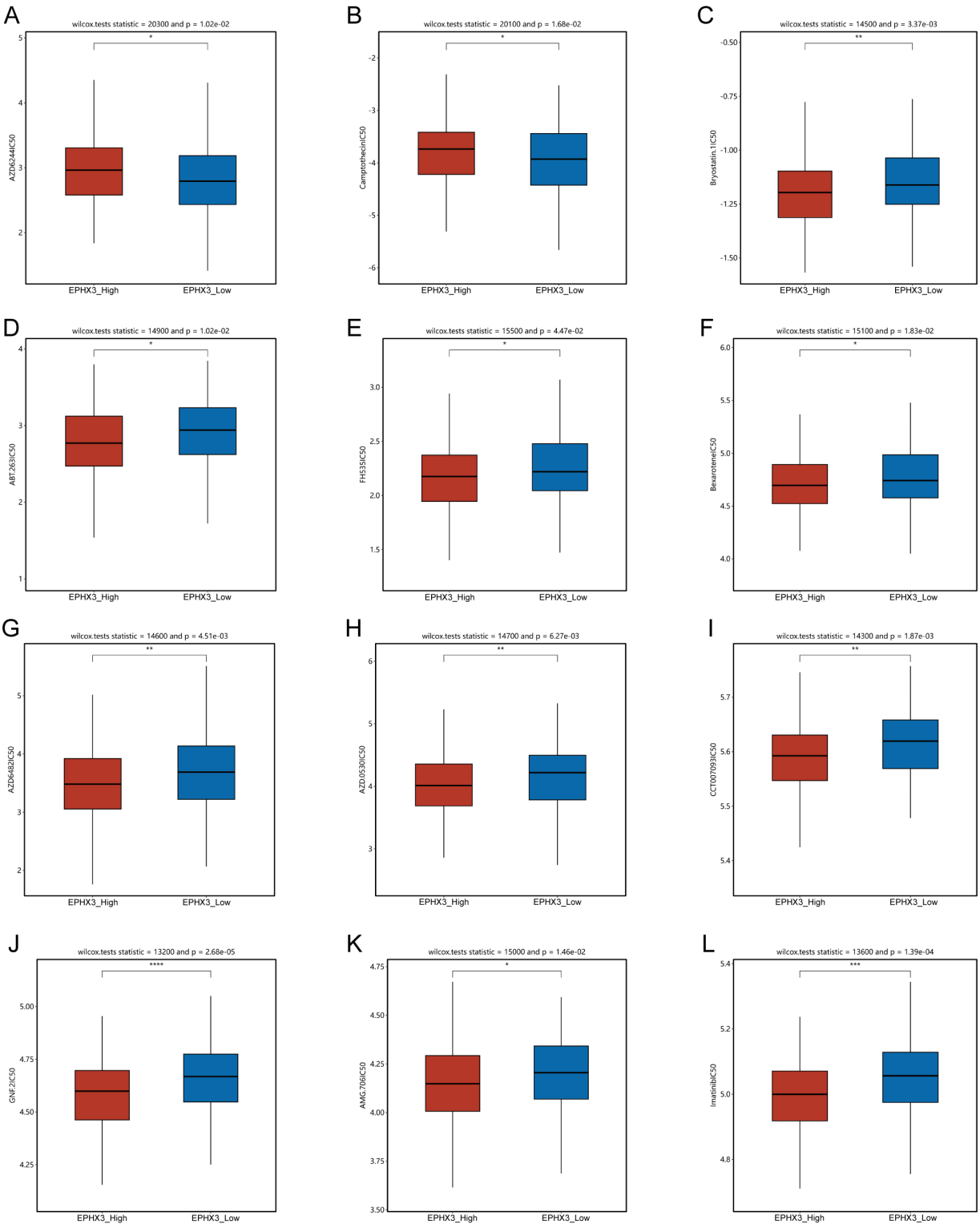


Figure 7

Association of EPHX3 expression levels with the sensitivity of GA to multiple antitumor drugs.

Supplementary Files

This is a list of supplementary files associated with this preprint. Click to download.

- SupplementaryMaterial1.pdf